

Hot-wire deposition of amorphous and microcrystalline silicon using different gas excitations by a coiled filament

Xunming Deng*, Henry S. Povolny

Department of Physics and Astronomy, University of Toledo, Toledo, OH 43606, USA

Abstract

Microcrystalline silicon ($\mu\text{c-Si:H}$) and amorphous silicon (a-Si:H) films were deposited using a hot-wire CVD (HWCVD) system that employs a coiled filament. Process gasses, H_2 and Si_2H_6 , could be directed into the deposition chamber via different gas inlets, either through a coiled filament for efficient dissociation or into the chamber away from the filament, but near the substrates. We found that at low deposition pressure (e.g. 20 mTorr) the structure of the films depends on the way gases are introduced into the hot-wire chamber. However, at higher pressure (e.g. 50 mTorr), Raman measurement shows similar results for films deposited with different gas inlets.

© 2003 Elsevier Science B.V. All rights reserved.

Keywords: Hot-wire deposition; Amorphous silicon; Microcrystalline silicon

1. Introduction

Hot-wire CVD has been demonstrated to have the potential to deposit a-Si:H and $\mu\text{c-Si:H}$ at higher rates than the widely used PECVD process (see for example [1]). It has also been found that the amount of hydrogen dilution needed to deposit $\mu\text{c-Si:H}$ in a HW process is significantly lower than in a PECVD process. However, few studies have been performed on the dependence of the deposition of silicon films on the geometry of the filament and the chamber, and the way process gases are directed into the deposition chamber. It is often pre-assumed that the properties and structure of the Si films deposited in HWCVD are independent of the way gases are directed into the chamber. In this paper, we report our study on the dependence of Si film structural properties on the flow schemes for direction of process gases into the chamber using a HWCVD process employing a coiled filament and multiple gas inlets.

2. Deposition chamber and experimental details

Fig. 1 is a schematic diagram of the HWCVD chamber with a coiled filament and three different gas inlets, showing, from top to bottom: heater; substrates; shutter;

top gas inlets; RF electrode; filament; and bottom gas inlet. The coiled filament is made of tungsten wire, 0.75 mm in diameter and approximately 1 m long, wound into a coil of ~ 7 mm in diameter and 5 cm long with 40 evenly spaced revolutions. Process gases, such as SiH_4 , GeH_4 , Si_2H_6 and H_2 , can flow into the chamber through any of the three inlets or any combinations of these inlets. The gas confinement cup is approximately 12.7 cm in diameter and 10 cm in height. It supports the two annular gas inlets (inlets 1 and 2), one even with the top of the hot wire coil and one 2.54 cm above the first. These move with the coil, such that the top annular gas inlet can be anywhere from approximately 1.3 to 3.5 cm from the substrate. The bottom gas inlet (inlet 3) is approximately 1 cm from the bottom of the coil. There is a shutter just a couple of mm below the substrate. Gases, directed through the inlet placed next to the heated filament (inlet 3, bottom inlet), interact with the filament many times, resulting in maximized dissociation. However, gases directed into the chamber near the substrates (inlets 1 and 2, top inlets) experience less catalytic reaction with the filament, but could be ‘remotely’ dissociated by the radicals generated near the filament.

The annular RF electrode is 11.4 cm in diameter and occupies the top 3.8 cm of the inside of the confinement cup. It is separated from the gas confinement cup by a ceramic spacer. Both the annular RF electrode and the

*Corresponding author. Tel.: +1-419-530-4782; fax: +419-530-2723.

E-mail address: dengx@physics.utoledo.edu (X. Deng).

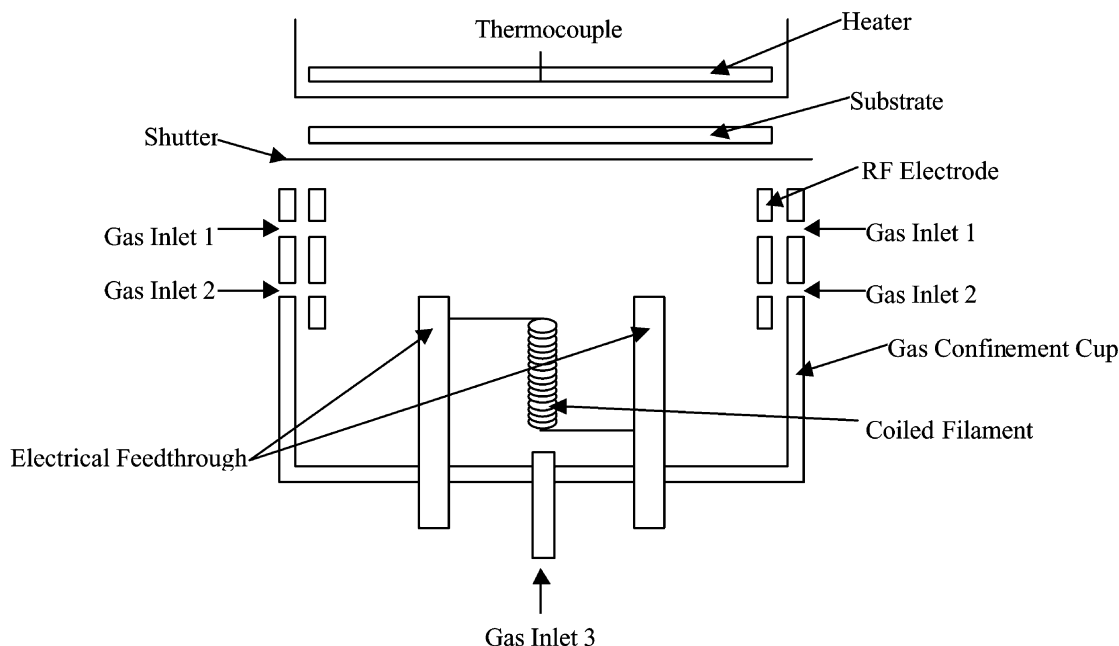


Fig. 1. Schematic diagram of the HWCVD chamber, showing the gas confining cup, multiple gas inlets, the coiled filament, RF electrode and some other details.

ceramic spacer have holes to allow the passage of gas from the two annular gas inlets. This electrode gives us the additional capability of employing a plasma-assisted HWCVD process. Some additional details of the HW chamber are provided elsewhere [2].

This HW deposition chamber is integrated into the University of Toledo's existing three-chamber PECVD system, routinely used for the fabrication of high-efficiency triple-junction solar cells [3]. The substrate can be transferred through gate valves between the HW chamber and the other three deposition chambers without an air break, allowing us to fabricate high-efficiency solar cell devices using the layers deposited in the HW chamber.

Two series of samples were prepared during this study. The first series of samples was prepared using HWCVD at different filament temperature T_{fil} and substrate temperature T_{sub} , with both Si_2H_6 and H_2 gases directed into the chamber from inlet 3. T_{sub} here is the temperature of the substrates (actually measured at the position of the heater) before the filament is turned on. The aim of the first sample series was to study the dependence of Si film structure on T_{fil} and T_{sub} for a fixed H dilution. The second series of samples was prepared at fixed T_{fil} and T_{sub} , but with different ways of directing gases into the chamber. A variety of substrates, including Corning 1737 glass, 7059 glass, quartz, crystalline silicon (c-Si) and stainless steel (SS), were used. The pressure was fixed at 20 mTorr for all samples. Raman spectra were measured using the 488-nm line of

a Coherent Innova 70 Ion Pure Plasma Tube argon laser using cylindrical focusing.

3. Results and discussion

3.1. HWCVD growth of $\mu\text{-Si:H}$ and $a\text{-Si:H}$ films at different T_{fil} and T_{sub}

Nine samples were deposited on various substrates at T_{fil} of 1700, 1900 and 2100 °C, and T_{sub} of 150, 225 and 300 °C. The other deposition conditions were: Si_2H_6 flow, 3 sccm; H_2 flow, 3 sccm; pressure, 20 mTorr; and total deposition time, 30 min. Both Si_2H_6 and H_2 were directed into the chamber via inlet 3 at the bottom. Fig. 2 shows the Raman scattering spectra for seven of these nine samples. Raman measurement could not be carried out for two samples deposited at $T_{fil} = 1700$ °C, since these films are too thin. The sharp peak near 520 cm^{-1} indicates that the Si material is microcrystalline, while a broad peak near 480 cm^{-1} indicates that the Si material is amorphous. Table 1 summarizes the Raman results for these samples. Comparing samples prepared at different T_{sub} , it is obvious that at lower T_{sub} , i.e. 150 and 225 °C, the material is more likely to be microcrystalline than samples deposited at 300 °C. Although sample HW23 is amorphous, while HW28 and HW30 are microcrystalline, we cannot conclude that the film structure depends on T_{sub} , since HW23 is much thinner than HW28 and HW30, and thinner samples are more likely to be amorphous. However, by

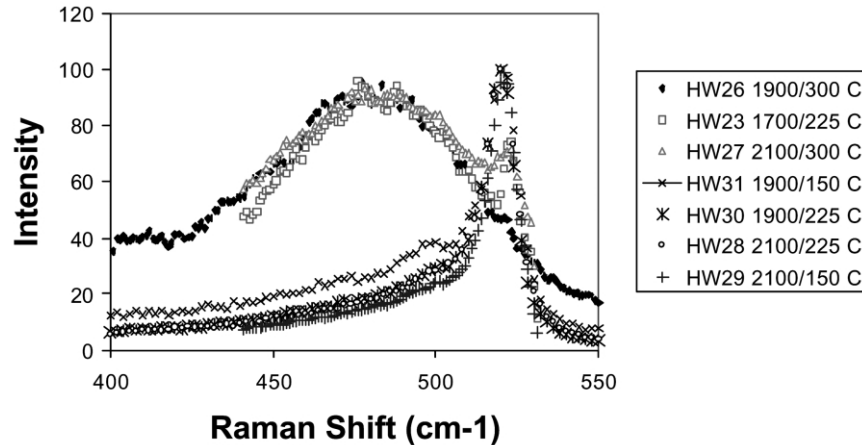


Fig. 2. Raman spectra for the HWCVD films deposited at different filament and substrate temperatures.

Table 1

Deposition conditions and Raman results for hot-wire films deposited at different filament and substrate temperatures

Sample	T_{fil} (°C)	T_{sub} (°C)	Thickness (nm)	Deposition rate (Å s ⁻¹)	Raman main peak (cm ⁻¹)	Structure
HW29	2100	150	970	5.4	520	Microcrystalline
HW28	2100	225	990	5.5	520	Microcrystalline
HW27	2100	300	1010	5.6	478	Amorphous
HW31	1900	150	1800	5.0	520	Microcrystalline
HW30	1900	225	2120	5.9	520	Microcrystalline
HW26	1900	300	2020	5.6	477	Amorphous
HW24	1700	150	180	0.5	Too thin	–
HW23	1700	225	250	0.7	476	Amorphous
HW25	1700	300	–	–	Too thin	–

Table 2

Deposition conditions and Raman scattering peaks for deposition with different gas-flow schemes

Sample	Si ₂ H ₆ flow	H ₂ flow	Thickness (nm)	Front surface		Back surface	
				Raman peaks (cm ⁻¹)	Structure	Raman peaks (cm ⁻¹)	Structure
HW28	Bottom inlet	Bottom inlet	990	519, 499	μc-Si:H	489	a-Si:H
HW37	Bottom inlet	Top inlet	1150	520, 499	μc-Si:H	519, 496	μc-Si:H
HW38	Top inlet	Bottom inlet	1050	520, 499	μc-Si:H	519, 497	μc-Si:H
HW39	Top inlet	Top inlet	1090	518, 499	μc-Si:H	489	a-Si:H

observing the relative intensity of the 520-cm⁻¹ peak, we find that HW27 has a higher volume fraction of microcrystalline phase than HW26. Therefore, it is likely that for our HWCVD design, higher T_{fil} favors microcrystalline formation. In addition to the peaks at 520 and 480 cm⁻¹, samples that show microcrystalline phase also show a small Raman peak at 500 cm⁻¹. This peak could be associated with Si having intermediate-range order [4] or Si near the grain boundaries.

3.2. Dependence of growth of μc-Si:H and a-Si:H on the gas flows in the HWCVD process

We selected sample HW28, deposited at $T_{\text{fil}}=2100$ °C and $T_{\text{sub}}=225$ °C, as a reference and deposited other samples under identical conditions, except that Si₂H₆ and H₂ gases were directed into the chambers through different inlets. Table 2 shows the flow schemes for four samples: HW28, HW37, HW38 and HW39. Other dep-

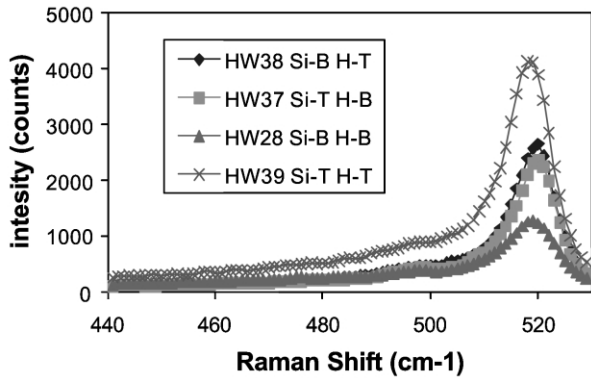


Fig. 3. Raman spectra measured from the front side of the samples.

osition conditions that were kept constant include: Si_2H_6 flow, 3 sccm; H_2 flow, 3 sccm; pressure, 20 mTorr; and time, 30 min. To study the microcrystallinity of these films with deposition time, Raman scattering was measured for the films deposited on quartz substrates on the front side (Fig. 3), as well as on the back side through the substrate (Fig. 4). Raman scattering measured from the front surface of the film reveals the structure of the material deposited during the final stage of deposition. In contrast, Raman scattering through the quartz substrate reveals the structure of the film deposited during the initial stage of the deposition. The front-surface Raman, shown in Fig. 2, shows that all samples are microcrystalline; only a sharp peak near 520 cm^{-1} and a small peak near 500 cm^{-1} are observed for each of the four samples. However, the backside Raman measurement shows quite a different structure among the four samples. Table 2 summarizes the Raman measurements from the front and back sides of the substrates. The Raman peak for a-Si:H is at 489 cm^{-1} rather than 480 cm^{-1} , possibly due to instrumentation drift.

From Figs. 2 and 3 and Table 2, we conclude that during the initial deposition on a quartz substrate, samples with Si_2H_6 and H_2 from separate inlets (one through the filament and one through a top inlet) show microcrystalline structure, while samples with both gases from the same inlet (through the filament or a top inlet) show amorphous structure. However, during the final stage of deposition (after 30 min), all samples show microcrystalline structure. This agrees with the suggestion by Collins et al. [5] that Si growth can become more microcrystalline when thickness builds up.

Let us now discuss the beginning stage of deposition. It would be expected that the initial layers of silicon are amorphous when grown on a quartz substrate, unless the growth conditions favor immediate nucleation of microcrystallites. It is not surprising that HW39 is amorphous during initial deposition when both gases are injected from inlet 1, since the amount of atomic H in the chamber is not expected to be more than that during

HW28 growth. It is also not hard to understand why HW38 is microcrystalline during initial growth, since the high concentration of atomic H remotely dissociates Si_2H_6 and generates SiH_3 radicals for Si growth. The ratio $[\text{atomic H}]/[\text{SiH}_3]$ is high in this case. However, it is against our intuition that HW37 is microcrystalline during initial growth, since there should be less atomic H in the chamber as compared with the growth of HW28. For that reason, we deposited another sample (HW46) under identical conditions as for HW37 and the same results were obtained. More study is needed to gain further understanding of Si growth in HWCVD when gases are injected into the chamber via separate inlets. One possible explanation is that a large amount of molecular H_2 also enhances microcrystalline formation.

We also prepared a set of four samples at a higher pressure of 50 mTorr, while the other conditions were kept the same. For all four samples, the initial deposition was amorphous and the final stage of deposition was microcrystalline. The difference due to the different gas flows disappears at higher deposition pressure.

4. Conclusions

We have deposited Si films at different T_{fil} and T_{sub} in a HWCVD chamber having a coiled filament. When both Si_2H_6 and H_2 are directed into the chamber through the filament coil, lower substrate temperature and higher filament temperature favor microcrystalline growth. The Si film structure depends on the way that process gases are directed into the HW chamber at low pressure (20 mTorr). Under certain conditions ($T_{\text{fil}} = 2000\text{ }^\circ\text{C}$, $T_{\text{sub}} = 225\text{ }^\circ\text{C}$, $P_r = 20\text{ mTorr}$, $\text{Si}_2\text{H}_6 = 3\text{ sccm}$ and $\text{H}_2 = 3\text{ sccm}$), the initial growth is amorphous, while the final growth stage is microcrystalline when both Si_2H_6 and H_2 are from the same inlet. In comparison, the initial growth is microcrystalline when Si_2H_6 and H_2 are injected into

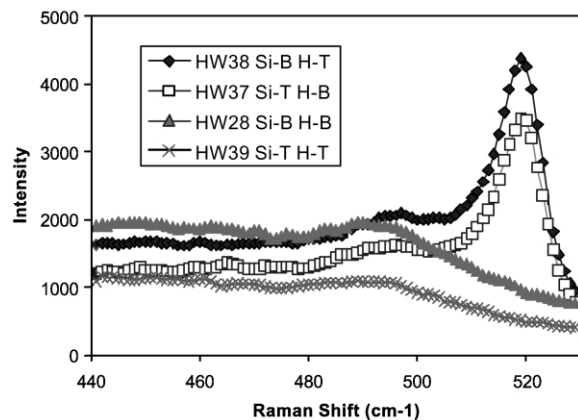


Fig. 4. Raman spectra measured from the back side through quartz substrates.

the chamber via different inlets, with one close to the filament and the other away from the filament. We think that the immediate formation of microcrystalline material when Si_2H_6 is from top inlet and H_2 is from bottom inlet is due to the favorable concentration of SiH_3 when Si_2H_6 is 'remotely' decomposed by atomic H generated by the hot filament. The immediate formation of microcrystalline phase using Si_2H_6 from the bottom inlet and H_2 from the top inlet is confirmed, but is not yet fully understood.

Acknowledgments

The authors would like to thank W. Du, X.B. Liao, W. Wang and X. Yang for experimental assistance and

A.H. Mahan for important discussions. This work was partially funded by the NREL Thin Film Partnership Program ZAF-8-17619-14 and NDJ-2-30630-08.

References

- [1] Proceedings of the 1st International Conference on Cat-CVD, 2000.
- [2] H.S. Povolny, X. Deng, *Thin Solid Films*, in press.
- [3] W. Wang, H. Povolny, W. Du, X. Liao, X. Deng, Proceedings of the 29th IEEE Photovoltaic Specialist Conference, 2002, p. 1082.
- [4] D.V. Tsu, B.S. Chao, S.R. Ovshinsky, S. Guha, J. Yang, *Appl. Phys. Lett.* 71 (1997) 1317.
- [5] A. Ferlauto, R. Koval, C. Wronski, R. Collins, *Appl. Phys. Lett.* 80 (2002) 2666.